# Soliton formation by interacting Airy beams

F. Diebel[a], D. V. Timotijević,[b] D. M. Jović Savić,[b] and C. Denz[a]

[a]*Institut für Angewandte Physik and Center for Nonlinear Science (CeNoS), Westfälische Wilhelms-Universität Münster, 48149 Münster, Germany*

[b]*Institute of Physics, University of Belgrade, P.O. Box 68, 11001 Belgrade, Serbia*

## ABSTRACT

In this contribution, we experimentally demonstrate a new type of spatial solitons arising from the mutual interaction of multiple two-dimensional Airy beams in a photorefractive nonlinear refractive index medium. Thereby, we combine two important concepts of optics: the fascinating accelerated Airy beams and nonlinear beam localization such as spatial soliton formation. We investigate the generation of this novel type of solitons and soliton pairs with respect to the number and phase relation of the superimposed Airy beams and support all experiments with comprehensive numerical simulations.

**Keywords:** Airy beams, Accelerated beams, Spatial Solitons, Nonlinear Photonics, Photorefractive Crystal, Spatial light modulators, Beam shaping

## 1. INTRODUCTION

Photonics and especially nonlinear photonics experience explosive growth during the last decade. Important roles in this development are played by the fascinating accelerated Airy beams on the one hand and by nonlinear effects such as soliton formation on the other. The potential arising from combining both topics to investigate nonlinear interaction of accelerated beams opens completely new aspects of research. The Airy function initially has been introduced by Berry and Balazs [1] as a free-particle solution of the nonlinear Schrödinger equation whose wave packet envelope shows two outstanding features: it stays unchanged and follows a parabolic trajectory while evolution – even without any external potential.

With the first realization of optical Airy beams [2,3] an active field of research was initiated, leading to a number of systematic investigations of the general properties of Airy beams in linear and nonlinear regimes. The unique ballistic-like, self-accelerating properties of the Airy beams moreover made them ideally suited for various applications ranging from micromanipulation, optical snow-blowers [4], all-optical routers [5], and even to ultra-fast self-accelerating pulses [6]. In the past, there have been many studies about the behavior of Airy beams in inhomogeneous refractive index potentials in order to shape beam caustics [7–9] and control the beam acceleration with linear refractive index gradients [10] or photonic lattices [11,12].

Nonlinearity adds another degree of freedom to the system and enables new dynamical propagation effects for the Airy beam as investigated in several experimental and theoretical studies [13–16]. In nonlinear systems, the formation of spatial solitons can be considered as one of the most fundamental effect which leads to localized structures that propagate unchanged, stabilized by the balanced interplay between diffraction and nonlinear self-focusing. In the field of optics, many soliton solutions in different systems have been reported, for example, bulk and discrete solitons [17–19], or vortex solitons [20,21]. Following, the fundamental question arises, if solitons or solitary structures can form from the interaction of initially accelerated beams such as Airy beams. First numerical works have started to explore the interaction between two one-dimensional Airy beams in an isotropic idealized nonlinear model [22–24].

In this contribution, we investigate the nonlinear interaction of two-dimensional Airy beams, and demonstrate a new type of spatial solitons arising from the mutual interaction of multiple two-dimensional Airy beams in a photorefractive nonlinear medium [25]. We show the generation of either solitons or soliton pairs depending on the number, phase configuration and beam intensity of the superimposed Airy beams and support all experiments with comprehensive numerical simulations. Furthermore, we investigate linear propagation of the synthesized

Author to whom correspondence should be addressed. Electronic mail: falko.diebel@uni-muenster.de

Complex Light and Optical Forces X, edited by Jesper Glückstad, David L. Andrews, Enrique J. Galvez, Proc. of SPIE Vol. 9764, 97640S · © 2016 SPIE
CCC code: 0277-786X/16/$18 · doi: 10.1117/12.2213527

beams and show tight-focus intensity structures resulting from interference. In this context, we employ advanced experimental methods to realize the compound optical field of accelerated Airy beams with fully controllable parameters and observe the nonlinear dynamics in a photorefractive nonlinear crystal. Our experimental setup offers unprecedented flexibility for precise and reproducible studies of nonlinear dynamics of Airy beams, but is not limited to this particular class of beams.

## 2. PHYSICAL MODEL AND NUMERICAL SIMULATIONS

We consider the scaled paraxial wave equation to describe the propagation of a monochromatic light field inside a nonlinear medium with intensity-dependent refractive index modulation. For the envelope $\psi$ of the optical field it reads as:

$$\mathrm{i}\frac{\partial\psi}{\partial\zeta} + \frac{1}{2}\left(\frac{\partial^2}{\partial\chi^2} + \frac{\partial^2}{\partial\nu^2}\right) + \frac{1}{2}k_0^2 w_0^2 \Delta n^2(I)\psi = 0. \tag{1}$$

In this equation, $\chi = x/\mathrm{w}_0$ and $\nu = y/\mathrm{w}_0$ are the dimensionless transverse coordinates scaled by the characteristic length $\mathrm{w}_0$ and $\zeta = z/k\mathrm{w}_0^2$ represents the dimensionless propagation distance with $k = 2\pi n/\lambda$.

In a photorefractive medium, the nonlinear material response causes an intensity-dependent refractive index modulation $\Delta n^2(I)$, with $I \propto |\psi|^2$. This nonlinearity is well approximated by the full anisotropic model, which describes the optical induction mediated by the electro-optic effect combined with the band transport model. For the optically induced space charge potential $\phi$ in a photorefractive SBN crystal with an applied electric field $E_{\mathrm{ext}}$ along the crystal's c-axis it reads as[26]

$$\nabla^2\phi + \nabla\ln(1+I)\cdot\nabla\phi = E_{\mathrm{ext}}\frac{\partial}{\partial x}\ln(1+I) + \frac{k_\mathrm{B}T}{e}\left(\nabla^2\ln(1+I) + (\nabla\ln(1+I))^2\right). \tag{2}$$

The refractive index modulation finally results directly from the electro-optic effect as $\Delta n^2 = n_0^4 r_{\mathrm{eff}}\partial_x\phi$, with $r_{\mathrm{reff}}$ being the effective electro-optic coefficient. This model also accounts for the orientation anisotropy caused by the directed transport of charge carriers, as well as the effect of charge carrier diffusion in the internal space charge field. For non-zero temperatures $T$ and non-zero dark conductivity of the crystal this leads to effects such as nonlinear soliton steering in bulk nonlinear media.

In the case of linear light propagation in a homogenous medium, the wave equation (1) can be separated into parts, each depending only on one transverse coordinate $\chi$ or $\nu$. The solution $\psi$ can be represented as a product of two one-dimensional functions $\varphi$ as

$$(\chi,\nu,\zeta) = \varphi(\chi,\zeta)\varphi(\nu,\zeta), \tag{3}$$

where $\zeta$ is the longitudinal coordinate. As introduced by Berry[1], a non-dispersive one-dimensional Airy function $\mathrm{Ai}(X)$ solves the individual part of the wave equation. Following the overall solution of the two-dimensional wave equation reads as:

$$(\chi,\nu,\zeta) = A_0\prod_{X=\{\chi,\nu\}}\mathrm{Ai}\left[X - \frac{\zeta^2}{4} + \mathrm{i}a_X\zeta\right]\exp\left[\frac{\mathrm{i}}{12}\left(6a_X^2\zeta - 12\mathrm{i}a_X X + 6\mathrm{i}a_X\zeta^2 + 6X\zeta - \zeta^3\right)\right]. \tag{4}$$

Here, $\mathrm{Ai}(X)$ denotes the Airy function, $A_0$ the amplitude and $a_X$ a positive decay length that truncates the solution to become physically relevant. Without this truncations the solution would be extended over the whole space and contains infinite energy. In the focal plane ($\zeta = 0$) the one-dimensional truncated function reads as $\varphi(X,0) = \mathrm{Ai}[X]\exp[a_X X]$, where an exponential decay clearly can be seen. These truncated solutions still solves the wave equation (1) and the distinguished properties of Airy beams are mostly preserved.[2]

To solve the paraxial wave equation (1) in the presence of an intensity-dependent refractive index modulation $\Delta n^2(I_{\mathrm{indu}})$ caused by nonlocal anisotropic photorefractive nonlinearity, numerical methods are required. Therefore, we have implemented comprehensive numerical routines based on split-step Fourier methods to evaluate the wave equation and simulate the beam propagation. The optically induced refractive index modulation needs to be calculated in each step. This means solving the potential equation of the full anisotropic model (2), which is done by using relaxation methods.

## 3. EXPERIMENTAL SETUP AND AIRY BEAM CHARACTERISTICS

Figure 1(a) shows a sketch of the experimental setup used for the presented experiments. The main components are a 20 mm long photorefractive nonlinear $Sr_{0.60}Ba_{0.40}Nb_2O_6$ (SBN:Ce) crystal and a programmable spatial light modulator (SLM) for the beam shaping. Light from a frequency-doubled Nd:$YVO_4$ laser ($\lambda = 532\,\mathrm{nm}$) illuminates the high-resolution phase-only SLM in reflection. The SLM imprints a specifically calculated spatial phase modulation onto the light field. In combination with two following lenses and a Fourier filter, this allows to shape any desired complex light field at the input face of the SBN crystal. With this approach, we could modulate amplitude and phase of the light field at the same time[27] and realize different complex light fields like combinations of multiple displaced two-dimensional Airy beams.

The SBN crystal is externally biased with an electric dc field of $E_{\mathrm{ext}} \approx 1000\,\mathrm{V\,cm^{-1}}$ aligned along the optical c-axis. To maximize the nonlinearity the beam is set to be extraordinarily polarized with respect to the crystal's optical c-axis. Due to the high electro-optic coefficient of SBN:Ce[28], sufficient nonlinearity results to substantially change the propagation of the Airy beam and enable the formation of spatial solitons. We can erase written refractive index modulations by illuminating the crystal homogeneously with white light. This reversibility makes our experimental approach highly flexible to perform series of experiments using the same nonlinear material.

Although the propagation characteristics of single Airy beams have been subject to many previous studies, we briefly want to recapitulate them to show the capabilities of the experimental setup to realize two-dimensional accelerated Airy beams with very high accuracy. As it is well known, Airy beams follows a parabolic trajectory while propagation in a linear, homogeneous environment. In the experimentally recorded pictures Figs. 1(b)–1(d) this behavior clearly can be seen. Figures 1(b) and 1(d) show the transverse intensity profile of the two-dimensional Airy beam at the front and the back face of the SBN crystal, respectively. The transverse displacement due to the accelerated propagation is clearly visible. A scan along the propagation direction verifies the parabolic trajectory of the beam, see Fig. 1(c).

To visualize the evolution of the intensity during propagation, we cut the recorded intensity volume along the coordinate in which the acceleration happens and show the cross-sections through it. It is worth to mention that recording the intensity inside the crystals is only possible if the refractive index between this plane and the camera is uniform, in other words, if the crystal is homogeneous.

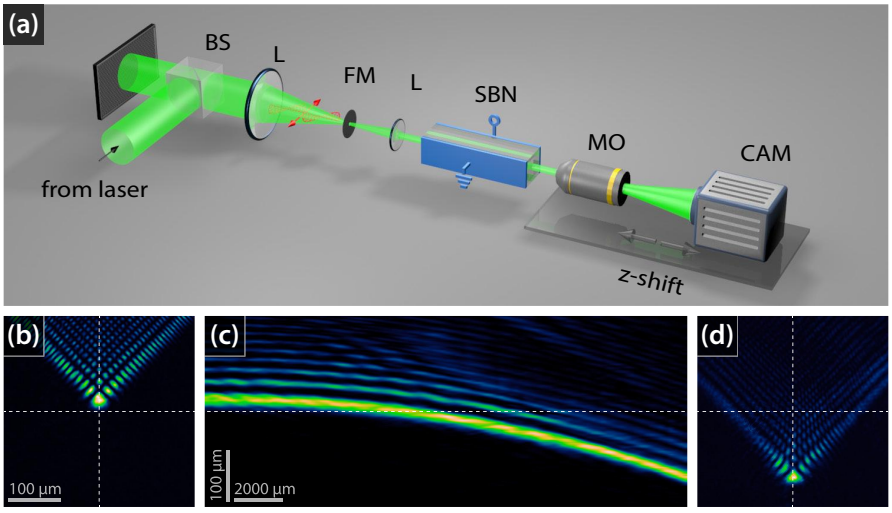


**Figure 1: Experimental setup and single Airy beam characteristics.** **(a)** Experimental setup (*SLM:* Spatial light modulator, *BS:* beam splitter, *FM:* Fourier mask, *SBN:* strontium barium niobate crystal, *MO:* microscope objective). **(b–d)** Linear propagation of a single two-dimensional Airy beam through the homogeneous crystal. **(b),(d)**: Intensity at the input and output face of the crystal, **(c)** cross-section during propagation.

## 4. INTERFERENCE OF MULTIPLE AIRY BEAMS DURING LINEAR PROPAGATION

To dive into the topic of multiple interacting Airy beams, we start with investigating the propagation of multiple Airy beams in the linear regime. In this case, the lack of nonlinearity prevents interaction between the beams, but interference already leads to interesting structures, including high-focusing beams. Since propagation is completely linear and the complex intensity patterns solely results from interference, their initial general accelerated trajectories are preserved, albeit the beam trajectories intersect. In all cases, the parabolic trajectories of the superimposed Airy beams can clearly be identified.

We start our studies with considering the most fundamental case of two co-propagating Airy beams coherently superimposed with an initial distance of $d \approx 50\,\mu\text{m}$. The beams are rotated by 180°, so that their accelerated trajectories will intersect during propagation. To tune the longitudinal position of the intersection there are two parameters to adjust. First, the size of the Airy beam which determines its curvature, and second, their initial spatial separation. We want to observe the intersection in the middle of the 20 mm long SBN crystal and therefore set the Airy beam size to $s \approx 25\,\mu\text{m}$, measured as the distance between the main lobe and the next neighbor.

Figures 2(a) and 2(b) show the experimental results for two propagating Airy beams, with the corresponding numerical simulations in Figs. 2(e) and 2(f). Thereby, we consider the two cases where the beams are either in phase, or $\pi$ out of phase, which result in distinguishable transverse intensity profiles during propagation due to interference. For the in-phase configuration (cf. Fig. 2(a,e)), interference leads to a very high local intensity in the intersection region of both accelerated trajectories compared to the surrounding. This feature previously was emphasized as the key advantage of so-called autofocusing beams [29,30]. In contrast, for the out-of-phase case (cf. Figs. 2(b,f)), destructive interference leads to a vertical separation by a dark line and no high-intensity focus is formed.

We now increase the number of superimposed beams to four. The most fundamental configuration is constructed with the four displaced Airy beams each rotated by 90°, as shown in Figs. 2(c,d,g,h). We want to limit our studies to the following two cases: either all beams are in phase (Figs. 2(c,g)), or neighboring beams are $\pi$ out of phase (Figs. 2(d,h)). However, in general there are more possibilities to chose the relative phases, e.g., to create vortex Airy beams.

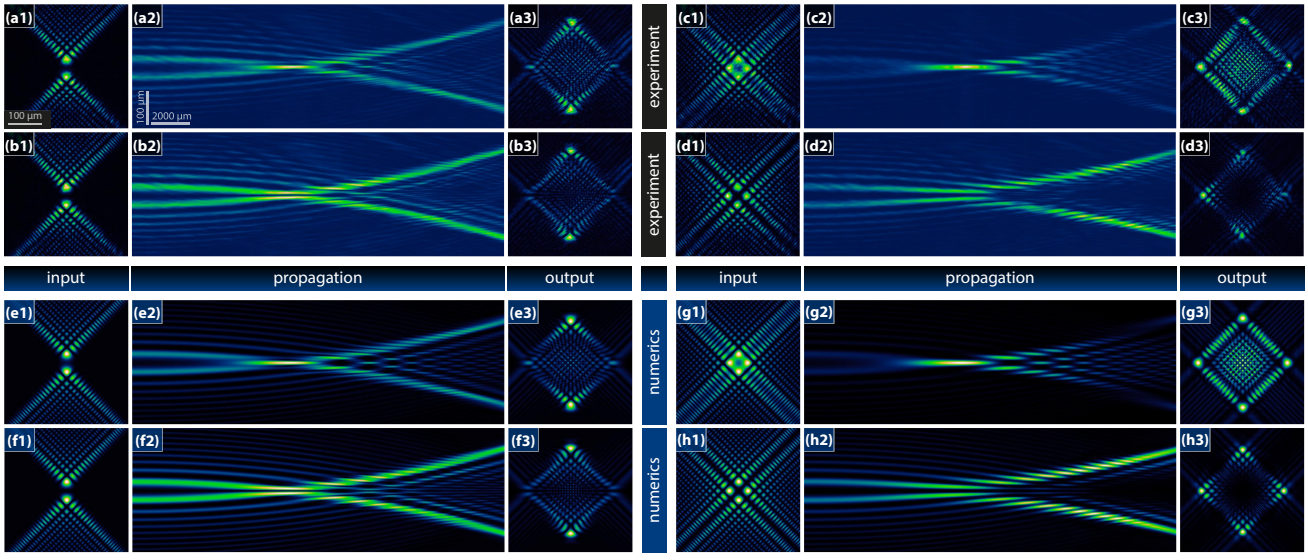


**Figure 2: Interference of multiple two-dimensional Airy beams in homogeneous linear medium.** **(a–d)** Experimental results for interfering Airy beams. **(e–h)** Corresponding numerical calculations. **(a,e)** Two beams in phase, **(b,f)** $\pi$ out of phase. **(c,g)** Four beams in phase, **(d,h)** $\pi$ out of phase. Each panel is normalized individually.

The longitudinal development of the intensity profile for four beams looks quite similar to case where two beams are superimposed, but the transverse intensity profiles now look quite different. The high-intensity focus for the in-phase case (cf. Fig 2(c,g)) is more pronounced as the number of interfering Airy beams are increased. The contrast between the focal intensity and the background continuously grows with the number of beams and achieves the limit when radially distributed Airy beams are superimposed [29].

For the propagation of multiple Airy beams in the linear regime the numerical results perfectly fits to the experimental measurements. Although the wave equation (1) for homogenous media ($\Delta n(I) = 0$) has analytical solution in form of truncated Airy beams which can be explicitly calculated for any distance $z$, we already here employ the numerical beam propagation method to prove and emphasize that the simulation methods we developed precisely describe the real experimental conditions.

## 5. NONLINEAR INTERACTION OF AIRY BEAMS

The results above show, that already interference led to fascinating intensity distributions, even without mutual interaction of the Airy beams. By including nonlinear light matter interaction, the beams will now influence each other and interesting novel nonlinear effects can be expected. For example, numerical studies predicted the formation of spatial solitons from two propagating Airy beams. [22,23]

Now, we systematically analyze and investigate the nonlinear propagation and interaction of multiple Airy beams in an SBN crystal. Here, the induced non-local refractive index modulation leads to a self-focusing saturable nonlinearity, resulting in completely changed propagation dynamics of the Airy beams. This enables fascinating new types of beam evolution and nonlinear effects that depends amongst others on the number of superimposed beams, their relative phase and intensity.

### 5.1 Nonlinear interaction of two Airy beams

First, we investigate the most fundamental configuration of two displaced Airy beams with the same parameters as described above for the linear case (cf. Fig. 2). The two beams are in phase, separated by $d \approx 50\,\mu\text{m}$ and rotated in this way that their trajectories would intersect in the linear case. We now increase the beam power to enter the nonlinear regime and to observe intensity dependent propagation dynamics. Thereby, we chose two different beam powers: $P_{\text{in}} \approx \{475,\ 1425\}\,\text{nW}$ and perform the experiment for each value, while keeping all other parameters such as external field, induction time, and background illumination unchanged.

Figure 3(a) shows the experimental and numerical results for the in-phase beam configuration. For low probe beam power, Fig. 3(a1) parts of the Airy beam are redirected to the center, other parts still follow the parabolic trajectory. While further increasing the probe beam power, we can see the transition to a well-localized solitary output state, see Figs. 3(a2). The solitary localized state emerges at the intersection of the Airy beams in the middle of the crystal, where constructive interference leads to a strongly increased local intensity. Afterwards, it propagates almost unchanged (except small breathing) due to the compensation of the diffraction by nonlinear self-focusing. The initial transverse momenta of the accelerated Airy beams now merges and compensate each other. Following, the formed solitary state propagates straight through the crystal.

Due to the merging of the individual beams, in peak intensity of the resulting state at the output is much higher than the peak intensity at the input. The ratio is given by the factor $r = I_{\text{max,out}}/I_{\text{max,in}}$ (see insets in Fig. 3) which helps to compare experiments and numerics more quantitatively. There is the principal limitation that direct imaging through a non-homogeneous medium is not possible. Therefore, only the output face of the SBN crystal is accessible for all nonlinear experiments.

We simulated the nonlinear propagation for different input intensities $I_{\text{in}} \approx \{0.65, 1.95\}$ according to the different probe beam powers in the experiment and could observe very good overall agreement with the experiments. The numerical simulations are shown in Figs. 3(b,c). The output profiles, as well as the intensity factor $r$ perfectly matches the real observations in experiment. This verifies that our implemented numerical methods exactly describe the real situation and justify to employ numerical simulations to get a detailed impression what dynamics happens during nonlinear propagation in the SBN crystal.

The formation of the solitary state is clearly visible if we look a the volumetric rendering of the numerically simulated intensity distribution during nonlinear propagation, see Fig. 3(c). The build-up process of the soliton

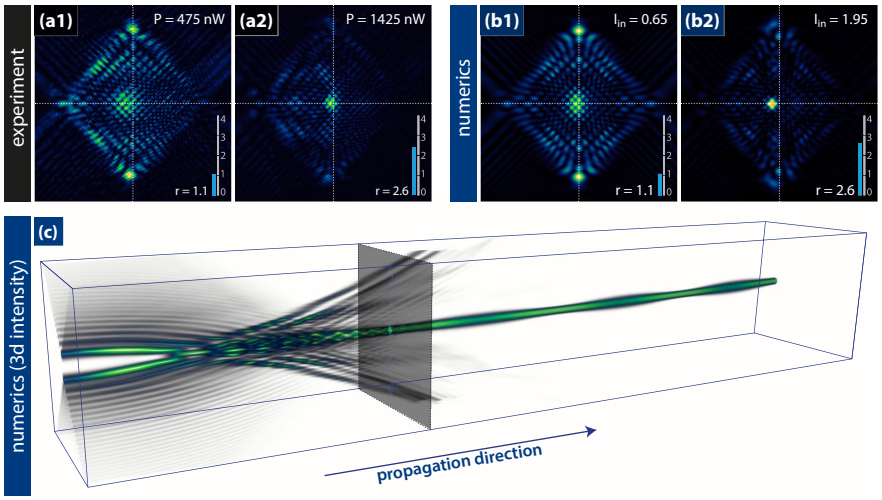


**Figure 3: Nonlinear interaction of two in-phase Airy beams. (a)** Experimental results for low and high probe beam power. The panels show the intensity pattern at the output face of the SBN crystal. **(b)** Results from corresponding numerical simulations. **(c)** Volumetric rendering of the numerically calculated intensity distribution (three times longer crystal) for strong nonlinearity. The position of the marked plane corresponds to the length of the used SBN crystal, $L = 20\,\text{mm}$ and to Figs. (a),(b). Each panel in normalized individually.

is accompanied by some modulations in the intensity and shape of the emerging state. After some propagation distance the remaining side lobes of the initial Airy beams vanishes and the system stabilizes. The solitary state now propagates almost unchanged, except small breathing. The length of the SBN crystal corresponds to the marked plane in Fig. 3(c).

In earlier studies, a similar localization behavior was also found numerically for simpler idealized isotropic Kerr, and saturable Kerr nonlinearities[23]. Here, for the experimental and numerical results in a photorefractive SBN crystal, the anisotropic, saturable and drift-dominated nonlinearity considerably complicated the situation. Additionally taking into account diffusion effects in the numerical model, allows us to explain the occurring slight transverse shift of the intensity peak in horizontal direction.

The situation is completely different for the other case, where the two Airy beams are $\pi$ out of phase. The results for this case are shown in Fig. 4. Due to the phase difference, destructive interference always separates the two main lobes of the initial Airy beams (c.f. Figs. 2(b) and 2(f)), consequently they do not merge. As a results, a pair of two localized solitary spots develops that propagates stably over large distances. Caused by the initial phase difference, these two solitons also have a phase difference of $\pi$ and hence repel each other, as reported for fundamental solitons[31]. The solitary states now propagate on straight lines which slowly diverge. This behavior can be nicely seen in Fig. 4(c). Not all parts of the Airy beams sufficiently interact and some parts of the beam remain unchanged. This disturbs the build-up process, but the remaining side lobes further follow their parabolic trajectory and quickly depart out of the volume. Consequently, the additional intensity modulations weaken and after a certain distance only small breathing remains.

## 5.2 Nonlinear interaction of four Airy beams

We now turn towards the more advanced case where four beams are synthesized. For four beams there are many different phase configuration. However, we restrict ourselves to the following two cases: either all beams are in phase, or with $\pi$ phase difference between neighboring beams. Again, we synthesize the beams in such a way that their trajectories will intersect, like in Fig. 2

The two different configurations now lead to completely different behavior. In the case, where all beams are in phase, the intensity again localizes in the middle with increasing probe beam power. Finally, a stable solitary state forms from the constructive interference of the beams in the region where their trajectories intersect. The

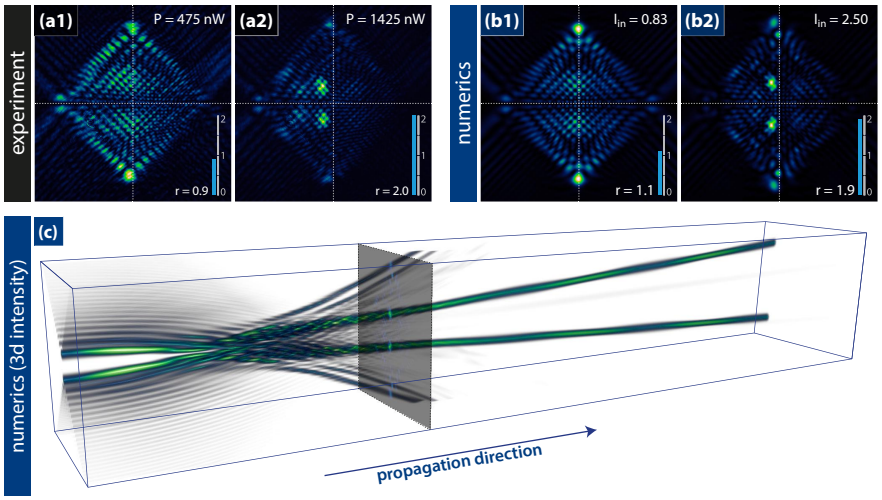


**Figure 4: Nonlinear interaction of two out-of-phase Airy beams.** **(a)** Experimental results for low and high probe beam power. The panels show the intensity pattern at the output face of the SBN crystal. **(b)** Results from corresponding numerical simulations. **(c)** Volumetric rendering of the numerically calculated intensity distribution (three times longer crystal) for strong nonlinearity. The position of the marked plane corresponds to the length of the used SBN crystal, $L = 20\,\text{mm}$ and to Figs. (a),(b). Each panel in normalized individually.

results are shown in Fig. 5(left). Since now four beams interfere, the transverse intensity pattern at the input face looks quite different, but we observe similar dynamics than for the corresponding two-beam case (c.f. Fig. 3). The experimental results for two different beam intensities $P_{\text{in}} \approx \{0.5, 3.0\}\,\mu\text{W}$ (Fig. 5(a)) clearly show the described formation of the solitary state as the transition from the four separated Airy main lobes (see Fig. 5(a1)) to the high-intensity localized state (see Fig. 5(a2)). Naturally, the ratio $r$ is much higher compared to the two-beam case, which is understandable because four beams are merging.

In the case of a phase difference of $\pi$ between neighboring beams, the situation is changed. Unlike the other presented cases, for this particular configuration no localized soliton or soliton pair is building, independent of the probe beam power. The corresponding experimental and numerical results are shown in Fig. 5(right). Due

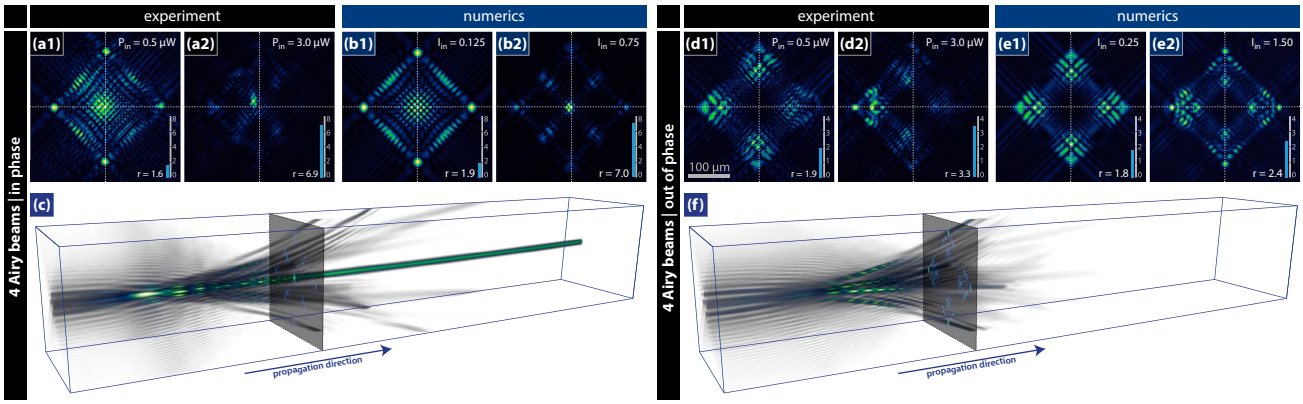


**Figure 5: Nonlinear interaction of four Airy beams.** **(left)** Formation of solitary state for in-phase case. **(right)** Nonlinear propagation for $\pi$ phase difference. **(a,d)** Experimental intensity pattern at the output face of the SBN crystal for different probe beam power. **(b,e)** Results from corresponding numerical simulations. **(c,f)** Volumetric plot of the three-dimensional intensity distribution (from numerics) for strong nonlinearity. Each panel is normalized individually.

to the mutual phase differences and the resulting destructive interference between the beams, no pronounces high-intensity region arises at the intersection of the trajectories. This prevents the formation of a single straight solitons. In addition, the noticeable remaining side lobes of the four Airy beams frustrate the build-up of a soliton pair, like it was observed for two Airy beams (cf. Fig. 4).

## Conclusion

In summary, we have demonstrated the intensity-dependent formation of solitons and soliton pairs from the nonlinear interaction of multiple accelerated Airy beams by systematically investigating their nonlinear dynamic for different configurations (e.g., number of beams, phase relation).

Comparing all results for two and four Airy beams, we could identify three different types of nonlinear dynamic. First, in both cases where the Airy beams are in phase, the interaction leads to the formation of a single stable solitary state emerged from the high intensity caused by constructive interference of the main lobes. In the opposite case, where the beams are $\pi$ out of phase, two other type of dynamical behavior could be observed. There is the formation of a soliton pair observed if two beams are superimposed with a phase difference of $\pi$. Finally, there is a third type if four Airy beams are superimposed with $\pi$ phase difference, where no solitary structures appear, even for the same intensities and nonlinearities. For this configuration the nonlinear dynamic shows symmetry-breaking behavior that depends critically on small perturbations and asymmetries in the system (e.g., directed diffusion of charge carriers).

Our highly-developed experimental platform enabled these fundamental results by performing nonlinear experiments with precisely shaped input beams and reproducibly controlled parameters, such as input beam power, external electric field, and illumination time. The presented methods and results will find applications in modern optical information processing architectures, while simultaneously enable further investigations about the interaction of other types of tailored optical beams (e.g. nondiffracting beams).

## References


[1] M. V. Berry and N. L. Balazs, Am. J. Phys. **47**, 264 (1979).
[2] G. A. Siviloglou and D. N. Christodoulides, Opt. Lett. **32**, 979 (2007).
[3] G. A. Siviloglou, J. Broky, A. Dogariu, and D. N. Christodoulides, Phys. Rev. Lett. **99**, 213901 (2007).
[4] J. Baumgartl, M. Mazilu, and K. Dholakia, Nat. Photonics **2**, 675 (2008).
[5] P. Rose, F. Diebel, M. Boguslawski, and C. Denz, Appl. Phys. Lett. **102**, 101101 (2013).
[6] A. Chong, W. H. Renninger, D. N. Christodoulides, and F. W. Wise, Nat. Photonics **4**, 103 (2010).
[7] N. K. Efremidis, Opt. Lett. **36**, 3006 (2011).
[8] N. K. Efremidis, Phys. Rev. A **89**, 023841 (2014).
[9] K. G. Makris, I. Kaminer, R. El-Ganainy, N. K. Efremidis, Z. Chen, M. Segev, and D. N. Christodoulides, Opt. Lett. **39**, 2129 (2014).
[10] S. Chávez-Cerda, U. Ruiz, V. Arrizón, and H. M. Moya-Cessa, Opt. Express **19**, 16448 (2011).
[11] N. M. Lučić, B. M. Bokić, D. Z. Grujić, D. V. Pantelić, B. M. Jelenković, A. Piper, D. M. Jović, and D. V. Timotijević, Phys. Rev. A **88**, 063815 (2013).
[12] F. Diebel, B. M. Bokić, M. Boguslawski, A. Piper, D. V. Timotijević, D. M. Jović, and C. Denz, Phys. Rev. A **90**, 033802 (2014).
[13] R. Bekenstein and M. Segev, Opt. Express **19**, 23706 (2011).
[14] Y. Hu, S. Huang, P. Zhang, C. Lou, J. Xu, and Z. Chen, Opt. Lett. **35**, 3952 (2010).
[15] Y. Hu, G. A. Siviloglou, P. Zhang, N. K. Efremidis, D. N. Christodoulides, and Z. Chen, *Nonlinear Photonics and Novel Optical Phenomena*, edited by Z. Chen and R. Morandotti, Springer Series in Optical Sciences, Vol. 170 (Springer New York, New York, NY, 2012).
[16] R. Driben, V. V. Konotop, and T. Meier, Opt. Lett. **39**, 5523 (2014).
[17] Y. S. Kivshar and G. P. Agrawal, *Optical Solitons: From Fibers to Photonic Crystals* (Academic Press, San Diego, 2003).
[18] C. Denz, M. Schwab, and C. Weilnau, *Transverse-Pattern Formation in Photorefractive Optics*, Springer Tracts in Modern Physics, Vol. 188 (Springer, Berlin, 2003).

[19] F. Lederer, G. I. Stegeman, D. N. Christodoulides, G. Assanto, M. Segev, and Y. Silberberg, Phys. Rep. **463**, 1 (2008).
[20] B. Terhalle, T. Richter, A. S. Desyatnikov, D. N. Neshev, W. Królikowski, F. Kaiser, C. Denz, Y. S. Kivshar, and W. Krolikowski, Phys. Rev. Lett. **101**, 013903 (2008).
[21] F. Diebel, D. Leykam, M. Boguslawski, P. Rose, C. Denz, and A. S. Desyatnikov, Appl. Phys. Lett. **104**, 261111 (2014).
[22] Y. Y. Zhang, M. R. Belić, Z. Wu, H. Zheng, K. Lu, Y. Li, and Y. Y. Zhang, Opt. Lett. **38**, 4585 (2013).
[23] Y. Zhang, M. R. Belić, H. Zheng, H. Chen, C. Li, Y. Li, and Y. Zhang, Opt. Express **22**, 7160 (2014).
[24] I. M. Allayarov and E. N. Tsoy, Phys. Rev. A **90**, 023852 (2014).
[25] F. Diebel, B. M. Bokić, D. V. Timotijević, D. M. Jović Savić, and C. Denz, Opt. Express **23**, 24351 (2015).
[26] A. A. Zozulya and D. Z. Anderson, Phys. Rev. A **51**, 1520 (1995).
[27] J. A. Davis, D. M. Cottrell, J. Campos, M. J. Yzuel, and I. Moreno, Appl. Opt. **38**, 5004 (1999).
[28] U. B. Dörfler, R. Piechatzek, T. Woike, M. K. Imlau, V. Wirth, L. Bohatý, T. Volk, R. Pankrath, and M. Wöhlecke, Appl. Phys. B Lasers Opt. **68**, 843 (1999).
[29] N. K. Efremidis and D. N. Christodoulides, Opt. Lett. **35**, 4045 (2010).
[30] D. G. Papazoglou, N. K. Efremidis, D. N. Christodoulides, and S. Tzortzakis, Opt. Lett. **36**, 1842 (2011).
[31] W. Królikowski, C. Denz, A. Stepken, M. Saffman, and B. Luther-Davies, Quantum Semiclassical Opt. J. Eur. Opt. Soc. Part B **10**, 823 (1998).